ACS Macro Letters

Letter

pubs.acs.org/macroletters

Photoselective Delivery of Model Therapeutics from Hydrogels

Donald R. Griffin and Andrea M. Kasko*

Department of Bioengineering, University of California—Los Angeles, 410 Westwood Plaza, 5121 Eng V, Los Angeles, California 90095, United States

Supporting Information

ABSTRACT: Hydrogels are commonly used in biomedical applications to sequester and release therapeutics. Covalently tethering therapeutic agents to a hydrogel through a degradable linkage allows their controlled release, but temporally separating the release of multiple therapeutics from a single hydrogel remains a major challenge. In this report, we use a series of photodegradable *ortho*-nitrobenzyl (*o*-NB) groups with varying structures to link model therapeutic agents (fluorescein, rhodamine, and amino-methylcoumarin acetate) to poly(ethylene glycol) macromers. We polymerized the macromers into hydrogel networks via redox polymerization and quantified the apparent rate constants of degradation (k_{app}) of each of the photoreleasable compounds. By exploiting differences in reactivity of the different *o*-NB groups, we are able to create complex, multistage release profiles. We demonstrate the ability to switch between concurrent and biased release of model therapeutics simply by switching wavelengths. We also demonstrate a complex four-stage release profile in which the release of three separate model therapeutics is controlled by varying wavelength, intensity, and exposure time. This is the first report of photoselective release of therapeutics from a hydrogel, allowing user-dictated real-time spatial and temporal control over *multiple* chemical signals in a cell microenvironment in 2D and 3D.

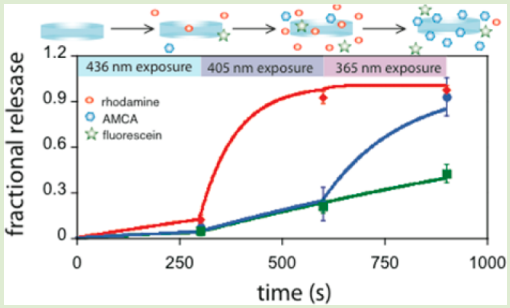

Hydrogels are commonly used as 3D scaffolds for cells, owing to their high water content and tunable physical properties. To use hydrogels to study cell differentiation and tissue evolution, it is critical to be able to deliver chemical cues in a well-defined manner.[1] Small and moderately sized therapeutics diffuse rapidly through hydrogels due to their highly swollen nature, so controlled delivery of these therapeutics is difficult to achieve without direct conjugation to the network. Covalently tethering therapeutic agents into a hydrogel through a degradable linkage allows control over their release. The two most common degradation mechanisms used for sustained release are hydrolysis and enzymolysis. In either mechanism, the rate of degradation cannot be adjusted or arrested once the material/scaffold is fabricated and implanted. Furthermore, in hydrolysis it is not possible to spatially control degradation as water is homogenously distributed throughout the sample. Enzymolysis is mediated by local enzyme concentration, and degradation typically occurs only in the area surrounding the cells due to limited lifetime and diffusivity of the enzyme in the network. As a result, neither hydrolysis nor enzymolysis allow both precise spatial and temporal control over release of signals, limiting the ability to recapitulate natural signaling cascades. In contrast to both hydrolysis and enzymolysis, photodegradation is externally controlled, allowing user-dictated on-demand release. Photochemistry has been established as an effective method to form biomaterials under physiological conditions,[2] used to uncage neurotransmitters,[3] used to spatially pattern chemical groups on and within[4−7] hydrogels, and used to pattern physical voids within a hydrogel,[8−11] all in the presence of live cells.[12]

We reported the synthesis and characterization of a model photoreleasable therapeutic agent using an *ortho*-nitrobenzyl (*o*-NB) ether linker as the photosensitive moiety. We quantified the effect of wavelength, light intensity, sample geometry, and exposure time on release of the therapeutic agent and developed and experimentally verified a predictive model of photodegradation.[13] Subsequently, Johnson et al. reported the photorelease of doxorubicin and camptothecin conjugated to polymer brushes through an *o*-NB linker.[14,15] These studies demonstrate the utility of photodegradation for controlled release of therapeutics from polymers and hydrogels.

While the delivery of a single therapeutic may be used for directing biological processes, the delivery of multiple therapeutics (simultaneous or staged) may provide more precise control over cell fate and tissue regeneration.[16−18] In the past decade, several research groups have reported the simultaneous and sequential delivery of therapeutics from scaffolds[19] by exploiting release kinetics of different hydrolytically degradable particles, each carrying a unique therapeutic payload.[16,17] Although these systems may be effective for simultaneous or sequential delivery, there is no way to externally control or alter the release kinetics once the construct has been fabricated. Furthermore, spatial control is only achieved through fabrication techniques and cannot be adjusted postfabrication.

Received: July 20, 2012
Accepted: October 12, 2012
Published: October 30, 2012

To achieve sequential delivery of therapeutics via photodegradation, we need a series of photodegradable groups with varying degradation kinetics. Recently, wavelength-selective peptide protecting groups[20,21] caged surfaces[22,23] and wavelength-orthogonal caged neurotransmitters[24] have been reported. Generally, photo-orthogonality is achieved by using chromophores with either distinct molar absorptivities or distinct quantum yields.[25] Because small modifications to the structure of the *o*-NB group significantly impact the absorptivity and photolysis rate,[26] we synthesized and characterized a series of *o*-NB linkers with a range of reactivities at varying wavelengths.[12] We incorporated each *o*-NB group into the backbone of PEG macromers and used hydrogels formed from these macromers to release encapsulated human mesenchymal stem cells, including the biased release of one cell population over another.[12] While these results are exciting, when the *o*-NB linker is incorporated into the backbone of the hydrogel network, only larger, physically entrapped species can be released in a controlled manner.

To demonstrate the utility of photodegradation for the staged release of multiple therapeutic agents from a single hydrogel depot, we synthesized model conjugates of different *o*-NB groups with varying photodegradation kinetics and molar absorptivities (Table 1). Starting with three of our previously

Table 1. Molar Absorptivities (ε) for *o*-NB Linkers and Apparent Rate Constants of Degradation (k_{app}, λ = 365 nm) for Their Fluorescein Conjugates

o-NB Linker

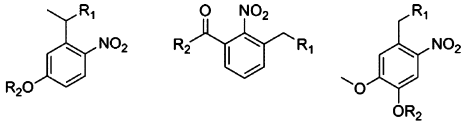

I II III

	I	II	III
$k_{app}/I_0 \times 10^4$ (cm^2/mW·s)	76.3	9.76	1.47
ε_{365nm} (M^{-1} cm^{-1})	2500 ± 93	150 ± 3.6	3400 ± 170
ε_{405nm} (M^{-1} cm^{-1})	161 ± 6.0	4.7 ± 0.26	730 ± 42
ε_{436nm} (M^{-1} cm^{-1})	2.7 ± 2.1	0.35 ± 0.21	56 ± 3.8
τ_{365nm} (min); I_0 = 5.53 mW/cm^2	0.395	3.09	20.5
τ_{405nm} (min); I_0 = 5.53 mW/cm^2	1.58	25.5	24.7
τ_{436nm} (min); I_0 = 5.53 mW/cm^2	45.3	164	154

reported *o*-NB intermediates (4-(4-(hydroxymethyl)-2-methoxy-5-nitrophenoxy)butanoic acid, 4-(3-(1-hydroxyethyl)-4-nitrophenoxy)butanoic acid, and 3-hydroxymethyl-2-nitrobenzoic acid), we brominated the benzylic alcohol of each *o*-NB group with phosphorus tribromide before aminating with ammonium hydroxide to yield a heterobifunctional linker (Schemes S1−S3). We protected the benzylic amine with di-*tert*-butyl dicarbonate and esterified the carboxylic acid with a polymerizable chain, poly(ethylene glycol) (PEG) methacrylate (M_n = 525). The *tert*-butyloxycarbonyl protecting group can be removed using trifluoroacetic acid in dichloromethane, but the other esters are simultaneously hydrolyzed, so we selectively deprotected the benzylic amine with bismuth trichloride.[27] We then coupled the amine of each *o*-NB linker to *N*-hydroxysuccinimide-functionalized fluorophores. We synthesized the fluorescein conjugate of each *o*-NB group to use for initial kinetic measurements, and we also conjugated each *o*-NB group to a unique fluorophore (fluorescein, rhodamine, and aminomethylcoumarin acetate (AMCA)) as models of different therapeutic agents (Figure 1). Notably, this conjugation approach results in direct release of the pure model therapeutic, with no fragments of the *o*-NB group (based on the degradation mechanism[28]).

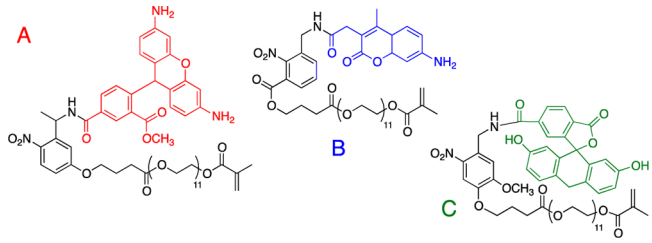

Figure 1. Model photoreleasable therapeutic agents. Conjugate A incorporates 4-(3-(1-hydroxyethyl)-4-nitrophenoxy) butanoic acid as the *o*-NB linker and releases rhodamine; conjugate B incorporates 3-hydroxymethyl-2-nitrobenzoic acid as the *o*-NB linker and releases AMCA; conjugate C incorporates 4-(4-(hydroxymethyl)-2-methoxy-5-nitrophenoxy) butanoic acid as the *o*-NB linker and releases fluorescein.

Although we previously quantified the degradation kinetics for the three *o*-NB linkers used in this study,[12] the different leaving group (amide vs benzyl ester) may alter the rate of degradation, as can the conjugation of a fluorophore to the releasable site of *o*-NB groups.[26] To quantify changes in the release kinetics due to these differences, we copolymerized each fluorescein-conjugated linker with PEG diacrylate (M_n = 4000) into a hydrogel, exposed the gels to light (λ = 365 nm, I_0 = 5.53 ± 0.14 mW/cm^2), and then quantified the amount of fluorescein released into solution via fluorescence. A semi-logarithmic plot of photodegradable group consumption as a function of exposure time (Figure S1) yields the apparent rate constant of photodegradation (k_{app}) for each *o*-NB conjugate (Table 1). There is approximately an order of magnitude difference in k_{app} between each *o*-NB conjugate, and k_{app} increases from almost 4- to 9-fold for each conjugate compared to their benzyl esters, indicating an influence of the fluorophore and leaving group on the degradation kinetics. We also calculated the characteristic degradation time ($\tau = 1/k_{app}$) for each linker at three different wavelengths utilized in this report (365 nm, I_0 = 5.53 mW/cm^2; 405 nm, I_0 = 21.1 mW/cm^2; 436 nm, I_0 = 44.6 mW/cm^2). At all wavelengths, the *o*-NB linker I has the shortest degradation time (τ_I = 24 s−45 min) and, thus, will always degrade first. *o*-NB linker II has a shorter degradation time than *o*-NB linker III at the highest energy light (τ_{II} = 3 min, τ_{III} = 20 min), but at longer wavelengths, *o*-NB linker III has slightly shorter degradation times than *o*-NB linker II (405 nm, τ_{III} = 24.7 min, τ_{II} = 25.5 min; 436 nm, τ_{III} = 154 min, τ_{II} = 164 min).

We first incorporated two model therapeutics (B and C) in equal concentration (10 μM) into a hydrogel. We exposed the gel first to λ = 405 nm (I_0 = 21.4 ± 1.1 mW/cm^2, t = 10 min) and subsequently to λ = 365 nm (I_0 = 5.53 ± 0.14 mW/cm^2, t = 10 min). Released fluorophores were leached from the gel between exposures. Figure 2 depicts the predicted (solid lines) and actual (data points) release of AMCA and fluorescein from the hydrogel. At the longer wavelength, there is no release bias for fluorescein or AMCA, but switching to higher energy light biases the release of AMCA over fluorescein. The actual release

dx.doi.org/10.1021/mz300366s | ACS Macro Lett. 2012, 1, 1330−1334

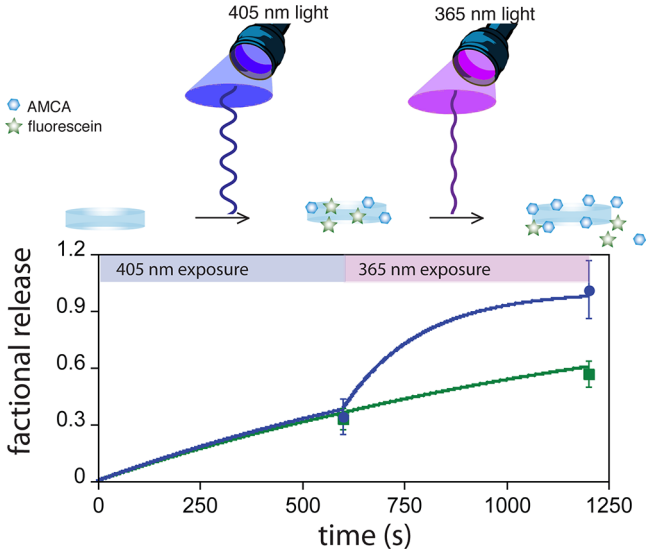

Figure 2. Fractional release of AMCA and fluorescein from a hydrogel as a function of light exposure (λ = 405 nm, I_0 = 21.4 ± 1.1 mW/cm^2, t = 10 min, then λ = 365 nm, I_0 = 5.53 ± 0.14 mW/cm^2, t = 10 min); solid lines depict predicted release, actual release shown as data points.

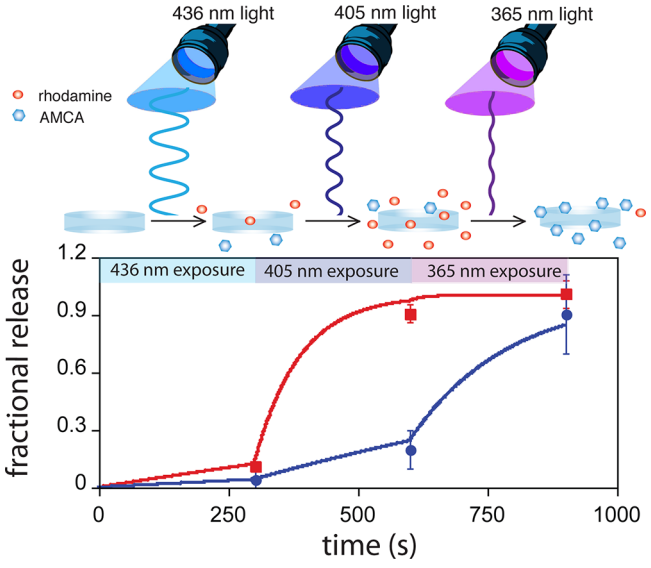

Figure 3. Fractional release of rhodamine and AMCA from a hydrogel as a function of light exposure (λ = 436 nm, I_0 = 44.6 ± 1.0 mW/cm^2, t = 5 min; λ = 405 nm, I_0 = 21.4 ± 1.1 mW/cm^2, t = 5 min; and then λ = 365 nm, I_0 = 5.53 ± 0.14 mW/cm^2, t = 5 min; solid lines depict predicted release, actual release shown as data points.

of AMCA and fluorescein matches the predicted release extremely well. Importantly, we have shown that it is possible to switch between an unbiased release profile (*o*-NB independent, at 405 nm) and a biased release profile (*o*-NB dependent, at 365 nm) simply by changing wavelengths. This is consistent with the calculated characteristic degradation times of *o*-NB linkers II and III, as at 405 nm τ_{II} and τ_{III} are very similar (~25 min), but at 365 nm, τ_{II} is an order of magnitude shorter than τ_{III} (τ_{II} = 3 min, τ_{III} = 20.5 min).

Next, we fabricated hydrogels containing A and B in equal concentrations (10 μM) and exposed the gels first to λ = 436 nm (I_0 = 44.6 ± 1.0 mW/cm^2, t = 5 min), then λ = 405 nm (I_0 = 21.4 ± 1.1 mW/cm^2, t = 5 min), and finally, to λ = 365 nm (I_0 = 5.53 ± 0.14 mW/cm^2, t = 5 min) (Figure 3). As predicted, at λ = 436 nm, the release of rhodamine (11%) is slightly biased over the release of AMCA (4.2%). At λ = 405 nm, we observe a drastic bias in the release of rhodamine (91%) over AMCA (20%). At the final exposure at λ = 365 nm, the remainder of the rhodamine is released, and most of the AMCA (90%) is released as well. These results demonstrate the ability to deliver therapeutics in a multistaged manner, releasing a bolus of one drug in one exposure (λ = 405 nm) and following its release with a second therapeutic at a subsequent exposure (λ = 365 nm). These results are also consistent with the calculated characteristic degradation times of *o*-NB linkers I and II, which predict that *o*-NB linker I (incorporated into conjugate A) will always degrade first. With decreasing wavelength, τ_{II} decreases, so the rate of release from conjugate B is expected to increase.

Finally, we incorporated all three conjugates (A–C) into a hydrogel in equal concentration (10 mM) and exposed the gels first to λ = 436 nm (I_0 = 44.6 ± 1.0 mW/cm^2, t = 5 min), then λ = 405 nm (I_0 = 21.4 ± 1.1 mW/cm^2, t = 5 min), and finally to λ = 365 nm (I_0 = 5.53 ± 0.14 mW/cm^2, t = 5 min; Figure 4). This light exposure program demonstrates a complex multistage delivery system: (stage 1) concomitant release of rhodamine, fluorescein and AMCA, with a slight bias toward rhodamine; (stage 2) heavily biased release of rhodamine over AMCA and fluorescein; (stage 3) biased release of AMCA over fluorescein; and (stage 4) reservoir of fluorescein accessible for

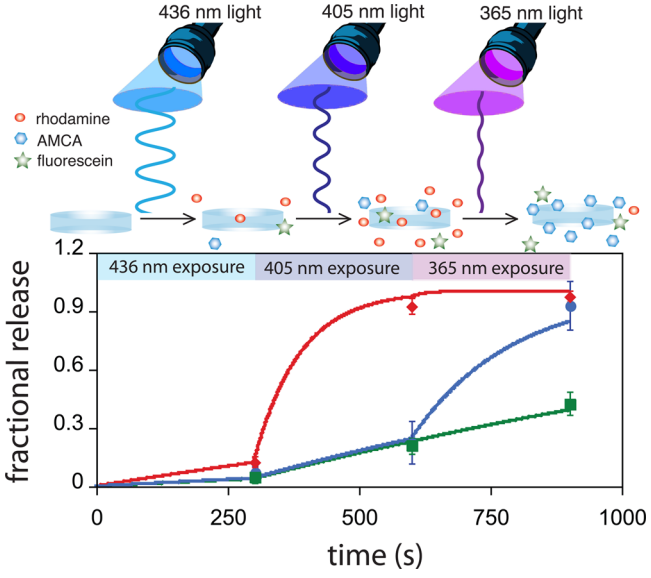

Figure 4. Fractional release of rhodamine, AMCA, and fluorescein from a hydrogel as a function of light exposure (λ = 436 nm, I_0 = 44.6 ± 1.0 mW/cm^2, t = 5 min; λ = 405 nm, I_0 = 21.4 ± 1.1 mW/cm^2, t = 5 min; and then λ = 365 nm, I_0 = 5.53 ± 0.14 mW/cm^2, t = 5 min); solid lines depict predicted release, actual release shown as data points.

subsequent release. Importantly, at the end of this specific light program, both rhodamine and AMCA are exhausted, leaving fluorescein conjugated to the hydrogel depot for release at a later stage. Again, the experimental data matches the model extremely well, and demonstrates that photodegradation can be used to achieve the multistaged release of three distinct therapeutics. All results are consistent with the calculated characteristic degradation times of all three *o*-NB linkers.

The correlation between the predicted and the actual release shown in all three figures demonstrates that photorelease is highly predictable and apparently independent of the number of photodegradable linkers (and therefore therapeutic agents).

dx.doi.org/10.1021/mz300366s | *ACS Macro Lett.* 2012, 1, 1330–1334

Because all three *o*-NB linkers absorb light and photodegrade at the target wavelengths, it is not possible to achieve completely selective release of one therapeutic over another using light alone. However, we clearly demonstrate that wavelength significantly impacts the relative release behavior, culminating in a multistaged release profile. Varying the concentration of each linker-therapeutic conjugate in the hydrogel, its distribution in the gel and the light program may further bias the release and allow selectivity, and light can be spatially controlled in 2D and 3D to achieve even more complex release profiles. Therefore, we have demonstrated that photodegradation is a useful method for precisely controlling the release of multiple signals and creating a complex cascade.

In conclusion, precise control over the properties of a biomaterial is critical to recapture the complex cascades of signals and complex microenvironments found in nature. In this report, we conjugated three model therapeutics (fluorescein, rhodamine and AMCA) to PEG macromers through photodegradable *o*-NB groups with varying structures. We quantified the molar absorptivities of each conjugate at three different wavelengths (365, 405, and 436 nm), polymerized the macromers into hydrogel networks via redox polymerization and quantified the apparent rate constants of degradation (k_{app}) of each of the photoreleasable compounds. By exploiting differences in reactivity of the *o*-NB groups, we created complex, multistage release profiles of the model therapeutics from hydrogels. Balancing the ratio of the rate constants of degradation, the number and concentration of therapeutics incorporated into gels and the light exposure program should allow temporally separated delivery of chemical signals with great precision. The ability to externally regulate different biological signals in a complex, spatiotemporally controlled manner will allow the elucidation of more complex relationships between biological signal presentation and cell and tissue response, and introduce a pathway to engineering complex tissues.

■ EXPERIMENTAL SECTION

Hydrogel Fabrication: Hydrogel disks were fabricated by dissolving PEG 4000 diacrylate (0.1 g, 24.3 μmol) in phosphate buffer (0.6 mL) before adding a predetermine number of fluorophore solutions (1 mM in DMSO, 0.01 mL each stock). DMSO was added to the solution (0.25 − 0.01 mL for each fluorophore included in hydrogel) to bring the total volume of DMSO in solution to 0.25 mL. Aliquots (0.075 mL) of APS (10 wt % in water) and TEMED (10 vol% in water) were added and vortexed sequentially. The solutions were then placed between two glass slides separated by two pieces of rubber (thickness = 0.5 mm) on either end and allowed to polymerize for 4 h, before removing from between the glass slides. Each hydrogel was cut into 5 mm discs and leached of unreacted material on a shaker plate. Sequential leaching order: DMSO/water (1:1, 3 × 250 mL), ethanol/water (1:1, 2 × 250 mL), water (1 × 250 mL), and phosphate buffer (3 × 250 mL). Following leaching each disk was placed individually into the well of a 24 well plate and covered with phosphate buffer (0.5 mL).

Measurement of Rate Constant of Degradation of *o*-NB Linker; Hydrogel Synthesis: Three sets of PEG 4000 diacrylate hydrogels (10 wt %) were copolymerized with the fluorescein conjugate derivative of each *o*-NB linker (0.01 mM). The hydrogels were polymerized and prepared as described above.

Degradation Procedure: Each set was exposed to light (λ = 365 nm, I_0 = 5.53 ± 0.14 mW/cm^2) for set periods of time. The times were determined based on the time required for complete degradation via photorheology (fluorescein conjugate of *o*-NB linker I: 10, 20, 30, 60, 120, 600 s; fluorescein conjugate of *o*-NB linker II: 1, 2, 3, 4, 5, 20 min; fluorescein conjugate of *o*-NB linker III: 1, 2, 3, 4, 5, 10, 30, 90 min). After exposure, the hydrogels were leached with phosphate buffer (0.5 mL) overnight. The solutions were then quantified using Tecan Plate Reader (λ_{ex} = 485 nm, λ_{em} = 535 nm).

Analysis Procedure: The fractional release profile of each linker was plotted on a semilog plot as a function of time. The slope of the curve was used to determine the apparent rate constant of degradation and the characteristic degradation time of each conjugate.

Photodegradation Model: Photodegradation was modeled numerically in MATLAB R2008b (The MathWorks, Inc., Natick, Massachusetts) at 365, 405, and 436 nm, as previously described.[12,13] The quantum yield φ of the photodegradable group at each wavelength was calculated from the empirical rate constants of photodegradation and the concentration, intensity, and wavelength at which those rate constants were obtained. For each time step of 1 s, the depth-dependent intensity of incident light was predicted by Euler integration of the spatial derivative of intensity in spatial steps of 1 μm. The absorptivities of the fluorescein-conjugate and its degraded products were used to model this attenuation of light. The rate of photodegradation was then recalculated at each depth using the intensity of light, the quantum yield φ, and the absorptivity of each linker. Euler integration of the time derivative of concentration of photodegradable group was used to model the conversion of undegraded to degraded linker. Release was predicted by multiplying the difference between the initial and final concentrations of undegraded linker at each depth by the volume of each spatial step and summing this quantity over the total volume of the gel.

Actual Photorelease from Multiconjugate Hydrogels; Exposure and Release Measurement of Hydrogel Depots Containing All Conjugates A−C: Three sets (N = 4) of hydrogels were exposed to 436 nm (44.6 ± 1.0 mW/cm^2) for 5 min. One set was then removed and DMSO (0.5 mL) was added to aid in leaching. The remaining two sets were exposed to 405 nm (21.4 ± 1.1 mW/cm^2) for 5 min. One set was then removed and DMSO (0.5 mL) was added to aid in leaching. The final set was exposed to 365 nm (5.53 ± 0.14 mW/cm^2) for 5 min. The final set was then removed and DMSO (0.5 mL) was added to aid in leaching. The released conjugates were measured by a Tecan plate reader (AMCA test: λ_{ex} = 360 nm, λ_{em} = 465 nm; fluorescein test: λ_{ex} = 485 nm, λ_{em} = 535 nm; rhodamine test: λ_{ex} = 535 nm, λ_{em} = 585 nm). A fourth set of hydrogels was left unexposed to determine the background signal for the samples. The fractional release was then determined by comparing the release of each experimental set (minus the background signal) to the signal (minus background) from a fifth set of hydrogels that was exposed to 365 nm light for 90 minutes; this represents complete release of all species from the hydrogel.

Exposure and Release Measurement of Hydrogel Depots Containing Conjugates B and C Only: Three sets (N = 4) of hydrogels were exposed to 436 nm (44.6 ± 1.0 mW/cm^2) for 5 min. One set was then removed and DMSO (0.5 mL) was added to aid in leaching. The remaining two sets were exposed to 405 nm (21.4 ± 1.1 mW/cm^2) for 5 min. One set was then removed and DMSO (0.5 mL) was added to aid in leaching. The final set was exposed to 365 nm (5.53 ± 0.14 mW/cm^2) for 5 min. The final set was then removed and DMSO (0.5 mL) was added to aid in leaching. The released conjugates were measured by a Tecan plate reader (AMCA test: λ_{ex} = 360 nm, λ_{em} = 465 nm; fluorescein test: λ_{ex} = 485 nm, λ_{em} = 535 nm; rhodamine test: λ_{ex} = 535 nm, λ_{em} = 585 nm). A fourth set of hydrogels was left unexposed to determine the background signal for the samples. The fractional release was then determined by comparing the release of each experimental set (minus the background signal) to the signal (minus background) from a fifth set of hydrogels that was exposed to 365 nm light for 90 min; this represents complete release of all species from the hydrogel.

Exposure and Release Measurement of Hydrogel Depots Containing Conjugates A and C Only: Two sets (N = 4) of hydrogels were exposed to 405 nm (21.4 ± 1.1 mW/cm^2) for 10 min. One set was then removed and DMSO (0.5 mL) was added to aid in leaching. The final set was exposed to 365 nm (5.53 ± 0.14 mW/cm^2) for 10 min. The final set was then removed and DMSO (0.5 mL) was added to aid in leaching. The released conjugates were measured by a Tecan plate

reader (AMCA test: λ_{ex} = 360 nm, λ_{em} = 465 nm; fluorescein test: λ_{ex} = 485 nm, λ_{em} = 535 nm; rhodamine test: λ_{ex} = 535 nm, λ_{em} = 585 nm). A third set of hydrogels was left unexposed to determine the background signal for the samples. The fractional release was then determined by comparing the release of each experimental set (minus the background signal) to the signal (minus background) from a fourth set of hydrogels that was exposed to 365 nm light for 90 minutes; this represents complete release of all species from the hydrogel.

■ ASSOCIATED CONTENT

Supporting Information

Experimental details and reaction schemes for synthesis and characterization of the *o*-NB fluorophore conjugates, degradation kinetics, and molar absorptivity. This material is available free of charge via the Internet at http://pubs.acs.org.

■ AUTHOR INFORMATION

Corresponding Author

*Tel.: +1 310 794 6341. Fax: +1 310 794 5956. E-mail: akasko@ucla.edu.

Notes

The authors declare the following competing financial interest(s): A.K. is a coinventor on U.S. Patent Application No. 11/374,471, which includes compounds described in this report.

■ ACKNOWLEDGMENTS

This work was funded by the National Institutes of Health through the NIH Director's New Innovator Award Program, 1-DP2-OD008533.

■ REFERENCES

(1) Lutolf, M. P.; Hubbell, J. a. *Nat. Biotechnol.* **2005**, *23* (1), 47−55.
(2) Bryant, S. J.; Nuttelman, C. R.; Anseth, K. S. *J. Biomater. Sci., Polym. Ed.* **2000**, *11* (5), 439−457.
(3) Wilcox, M.; Viola, R. W.; Johnson, K. W.; Billington, A. P.; Carpenter, B. K.; Mccray, J. A.; Guzikowski, A. P.; Hess, G. P. *J. Org. Chem.* **1990**, *55* (5), 1585−1589.
(4) Hahn, M. S.; Miller, J. S.; West, J. L. *Adv. Mater.* **2006**, *18* (20), 2679−2684.
(5) Hahn, M. S.; Taite, L. J.; Moon, J. J.; Rowland, M. C.; Ruffino, K. A.; West, J. L. *Biomaterials* **2006**, *27* (12), 2519−2524.
(6) Luo, Y.; Shoichet, M. S. *Nat. Mater.* **2004**, *3* (4), 249−253.
(7) Luo, Y.; Shoichet, M. S. *Biomacromolecules* **2004**, *5* (6), 2315−2323.
(8) Kloxin, A. M.; Kasko, A. M.; Salinas, C. N.; Anseth, K. S. *Science* **2009**, *324* (5923), 59−63.
(9) Kloxin, A. M.; Tibbett, M. W.; Kasko, A. M.; Fairbairn, J. A.; Anseth, K. S. *Adv. Mater.* **2010**, *22* (1), 61−66.
(10) Wong, D. Y.; Griffin, D. R.; Reed, J.; Kasko, A. M. *Macromolecules* **2010**, *43* (6), 2824−2831.
(11) Sarig-Nadir, O.; Livnat, N.; Zajdman, R.; Shoham, S.; Seliktar, D. *Biophys. J.* **2009**, *96* (11), 4743−4752.
(12) Griffin, D. R.; Kasko, A. M. *J. Am. Chem. Soc.* **2012**, *134* (31), 13103−13107.
(13) Griffin, D. R.; Patterson, J. T.; Kasko, A. M. *Biotechnol. Bioeng.* **2010**, *107* (6), 1012−1019.
(14) Johnson, J. A.; Lu, Y. Y.; Burts, A. O.; Lim, Y.-H.; Finn, M. G.; Koberstein, J. T.; Turro, N. J.; Tirrell, D. A.; Grubbs, R. H. *J. Am. Chem. Soc.* **2010**, *133* (3), 559−566.
(15) Johnson, J. A.; Lu, Y. Y.; Burts, A. O.; Xia, Y.; Durrell, A. C.; Tirrell, D. A.; Grubbs, R. H. *Macromolecules* **2010**, *43* (24), 10326−10335.
(16) Simmons, C. A.; Alsberg, E.; Hsiong, S.; Kim, W. J.; Mooney, D. J. *Bone* **2004**, *35* (2), 562−569.
(17) Richardson, T. P.; Peters, M. C.; Ennett, A. B.; Mooney, D. J. *Nat. Biotechnol.* **2001**, *19* (11), 1029−1034.
(18) Burdick, J. A.; Mason, M. N.; Hinman, A. D.; Thorne, K.; Anseth, K. S. *J. Controlled Release* **2002**, *83* (1), 53−63.
(19) Chen, F. M.; Zhang, M.; Wu, Z. F. *Biomaterials* **2010**, *31* (24), 6279−6308.
(20) Kotzur, N.; Briand, B.; Beyermann, M.; Hagen, V. *J. Am. Chem. Soc.* **2009**, *131* (46), 16927−16931.
(21) Hagen, V.; Kotzur, N.; Briand, B.; Beyermann, M. *Amino Acids* **2009**, *37*, 43−43.
(22) San Miguel, V.; Bochet, C. G.; del Campo, A. *J. Am. Chem. Soc.* **2011**, *133* (14), 5380−5388.
(23) Stegmaier, P.; Alonso, J. M.; del Campo, A. *Langmuir* **2008**, *24* (20), 11872−11879.
(24) Stanton-Humphreys, M. N.; Taylor, R. D. T.; McDougall, C.; Hart, M. L.; Brown, C. T. A.; Emptage, N. J.; Conway, S. J. *Chem. Commun.* **2012**, *48* (5), 657−659.
(25) Blanc, A.; Bochet, C. G. *Org. Lett.* **2007**, *9* (14), 2649−2651.
(26) Zhao, Y. R.; Zheng, Q.; Dakin, K.; Xu, K.; Martinez, M. L.; Li, W. H. *J. Am. Chem. Soc.* **2004**, *126* (14), 4653−4663.
(27) Navath, R. S.; Pabbisetty, K. B.; Hu, L. Q. *Tetrahedron Lett.* **2006**, *47* (3), 389−393.
(28) Gaplovsky, M.; Il'ichev, Y. V.; Kamdzhilov, Y.; Kombarova, S. V.; Mac, M.; Schworer, M. A.; Wirz, J. *Photochem. Photobiol. Sci.* **2005**, *4* (1), 33−42.